

Optical bistability on a silicon chip

Vilson R. Almeida and Michal Lipson

School of Electrical and Computer Engineering, Cornell University, 411 Phillips Hall, Ithaca, New York 14853

Received April 27, 2004

We demonstrate, for the first time to our knowledge, optical bistability on a highly integrated silicon device, using a 5- μm -radius ring resonator. The strong light-confinement nature of the resonator induces nonlinear optical response with low pump power. We show that the optical bistability allows all-optical functionalities, such as switching and memory with microsecond time response and a modulation depth of 10 dB, driven by pump power as low as 45 μW . Silicon optical bistability relies on a fast thermal nonlinear optical effect presenting a 500-kHz modulation bandwidth. © 2004 Optical Society of America
 OCIS codes: 130.3120, 130.4310, 190.1450, 230.1150, 230.3120.

Silicon is the dominant material in the microelectronic industry and is increasingly being considered as a platform for photonic integrated circuits.^{1,2} Passive Si photonic devices that bend, split, couple, and filter light have recently been demonstrated³; their optical properties are predetermined by design and fabrication. Active Si photonic devices in which light is controlled by light are a long-standing goal in all-optical communication but are challenging because of the relatively weak Si nonlinear optical properties.⁴ Optical bistability can be employed to allow all-optical functionalities, such as logic functions, modulation, switching, and memory⁵; it has been achieved in compound semiconductor materials with strong nonlinear optical properties.⁵⁻⁷ One can achieve optical bistability on Si by exploiting its thermal nonlinear optical effect,⁵ because of its large thermo-optic coefficient $\partial n/\partial T = 1.86 \times 10^{-4} \text{ K}^{-1}$ (Ref. 8); however, it has been demonstrated only in large structures with high pump powers.⁵

Here we demonstrate optical bistability on a compact micrometer-size Si integrated structure using input optical powers around 1 mW. The structure, a ring resonator,^{9,10} provides strong light confinement that allows both the miniaturization of device dimensions and the observation of optical bistability with relatively low optical pump power.

Figure 1 shows the laterally coupled 5- μm -radius ring resonator based on silicon-on-insulator (SOI) technology. We fabricated the structures on the SOI platform by using the same fabrication parameters as described in a recent work.¹¹ The rectangular cross section of both ring and waveguide is 450 nm wide by 250 nm high. Figure 2 shows the quasi-TE transmission of the ring resonator, where the quasi-TE mode is characterized by the electric field oriented predominantly along the plane of the substrate. Two resonances are shown, at $\lambda_{\text{resA}} = 1561.87 \text{ nm}$ and $\lambda_{\text{resB}} = 1580.04 \text{ nm}$, with full width at half-maximum linewidths of $\Delta\lambda_{\text{resA}} = 0.11 \text{ nm}$ and $\Delta\lambda_{\text{resB}} = 0.20 \text{ nm}$, respectively, corresponding to resonator quality factors of $Q_{\text{resA}} = 14,200$ and $Q_{\text{resB}} = 7900$, respectively. Total insertion losses at off-resonance condition were found to be 5 dB for a 7-mm-long waveguide terminated on nanotapers and light coupled through a tapered-lensed fiber.¹¹

To demonstrate optical bistability with the ring resonator, we used a pump wavelength slightly above λ_{resA} ($\lambda_0 = 1562.0 \text{ nm}$) and measured the transmitted power while varying the input power. As the input power is modified, the ring resonance shifts due to the thermo-optic effect in Si, thereby modifying the ring resonator transmittance. The resonance shift strongly depends on the circulating optical power inside the ring, which in turn strongly depends on the wavelength detuning between the optical source and the shifted resonance; the combined effect of these interrelated mechanisms leads to the bistability curve.⁵ Figure 3 shows the measured clockwise hysteresis loop, which evidences a strong optical bistability effect⁵; the insets show where the pump wavelength is located relative to the resonance for three distinct positions in the hysteresis loop.

To determine the modulation bandwidth of the ring resonator, we used a pump-probe experimental setup in which the pump and probe wavelengths were set on the long-wavelength edge of the resonances at λ_{resA} and λ_{resB} , respectively. We modulated the pump input power with a sinusoidal signal with peak amplitude of 40 μW superposed to a cw bias of 100 μW and measured the output modulation of the probe, which was driven by a 50- μW cw input. We obtained a 3-dB modulation bandwidth of 500 kHz.

The most direct application of optical bistability is in all-optical memory.⁵ To demonstrate this functionality, we show in Fig. 4 switching of the output power between two stable states by modulation of the

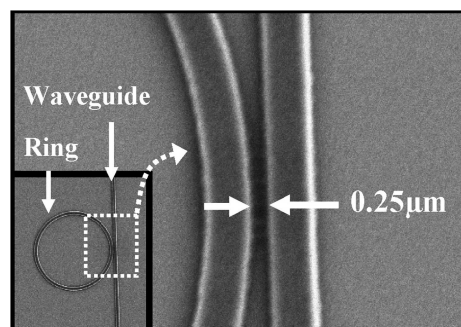


Fig. 1. Scanning electron micrograph of a Si ring resonator laterally coupled to a single waveguide.

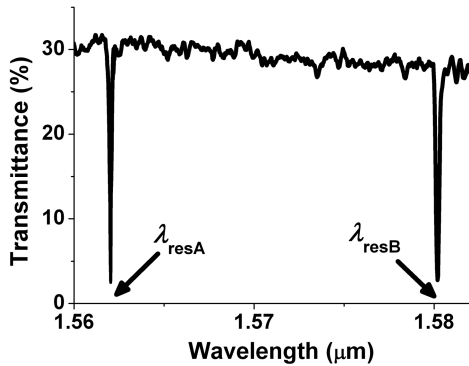


Fig. 2. Transmittance spectrum of the quasi-TE mode of a Si ring resonator showing only two of its resonances: $\lambda_{\text{resA}} = 1561.87$ nm and $\lambda_{\text{resB}} = 1580.04$ nm.

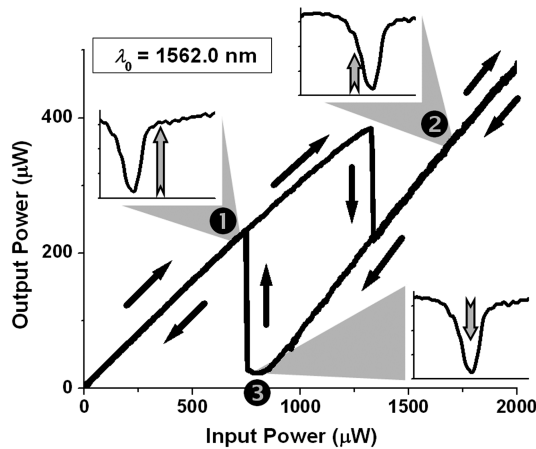


Fig. 3. Hysteresis curve for the quasi-TE mode of a SOI ring resonator excited at $\lambda_0 = 1562.0$ nm. Markers define curve points related to the transmission spectra in the insets: ① unshifted spectrum on the linear region before hysteresis loop, ② shifted spectrum due to high-input increasing power, ③ resonance shifted to pump wavelength.

input power. The inset in Fig. 4 shows the hysteresis loop at the wavelength of operation, $\lambda_0 = 1562.0$ nm. The input power is set initially to a value inside the hysteresis loop ($P_{\text{in}} = 800$ μW , marker ①). Increasing the input power to a value outside the loop ($P_{\text{in}} = 1600$ μW , marker ②) and then decreasing it back to $P_{\text{in}} = 800$ μW (marker ③) shifts the output power from a high-output state ($P_{\text{out}} = 250$ μW , marker ①) to a low-output state output ($P_{\text{out}} = 25$ μW , marker ③). To switch the output power back to its high-output state, the input power is slightly decreased to $P_{\text{in}} = 700$ μW (marker ④) and then increased back to $P_{\text{in}} = 800$ μW (marker ① again), completing the hysteresis loop. The output modulation depth between the two stable states is 10 dB. The measurements of all-optical memory behavior show excellent agreement with the predictions based on the bistability model, which were obtained by projecting the input power signal (lower plot in Fig. 4) onto the hysteresis loop (x axis of Fig. 3) and extracting the corresponding output level (y axis of Fig. 3).

The optical bistability can also be used for all-optical switching. We performed a pump-probe experiment

in which optical bistability induced by the high-power pump was used to achieve switching of the low-power probe. Pump and probe wavelengths were set near the resonances shown in Fig. 2, $\lambda_{\text{pump}} = 1561.96$ nm and $\lambda_{\text{probe}} = 1580.24$ nm. The inset in Fig. 5 shows the hysteresis loop for $\lambda_{\text{pump}} = 1561.96$ nm. Notice that the hysteresis loop for this wavelength is narrower than that for $\lambda_{\text{pump}} = 1562.0$ nm (shown in Fig. 3); therefore it is more appropriate for all-optical switching with low pump power levels. The pump power was modulated by a square wave such that its low- and high-input levels lie outside the hysteresis loop range for $\lambda_{\text{pump}} = 1561.96$ nm (see Fig. 5, markers ① and ②, respectively). Figure 5 shows both pump and probe output curves as a result of 100-kHz modulation of the input pump power. The modulation amplitude of the input pump power required for switching the probe between the two states with a modulation depth of 8 dB was 250 μW . To further decrease this power level, we also used an alternative modulation scheme in which the pump power comprises two optical sources: a bias beam providing a constant high power at $\lambda_{\text{bias}} = 1561.96$ nm and a control beam providing a modulated low power at $\lambda_{\text{ctrl}} = \lambda_{\text{resA}} = 1561.87$ nm. The probe beam is again set at $\lambda_{\text{probe}} = 1580.24$ nm. The bias beam is set to a level slightly below the hysteresis loop (see Fig. 5, marker ①), such that a relatively small control power is needed to cause the system to undergo strong output switching. We find that, by using a bias power of 550 μW , a control beam power modulated between 0 and 45 μW is sufficient to attain switching of the probe beam with an approximately 10-dB modulation depth.

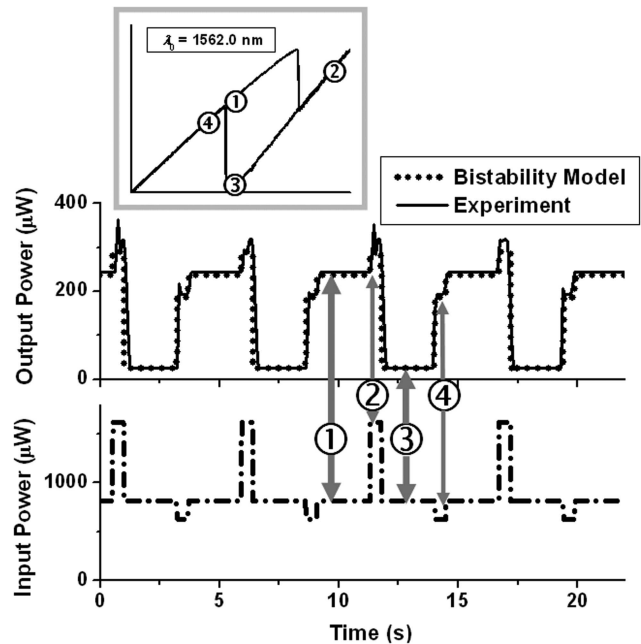


Fig. 4. All-optical memory functionality on a Si ring resonator driven by optical bistability at $\lambda_0 = 1562.0$ nm. Inset, hysteresis curve. Markers make links between the bistability curve and time-domain plots: ① high-output state, $P_{\text{in}} = 800$ μW ; ② high-to-low transient, $P_{\text{in}} = 1600$ μW ; ③ low-output state, $P_{\text{in}} = 800$ μW ; ④ low-to-high transient, $P_{\text{in}} = 700$ μW .

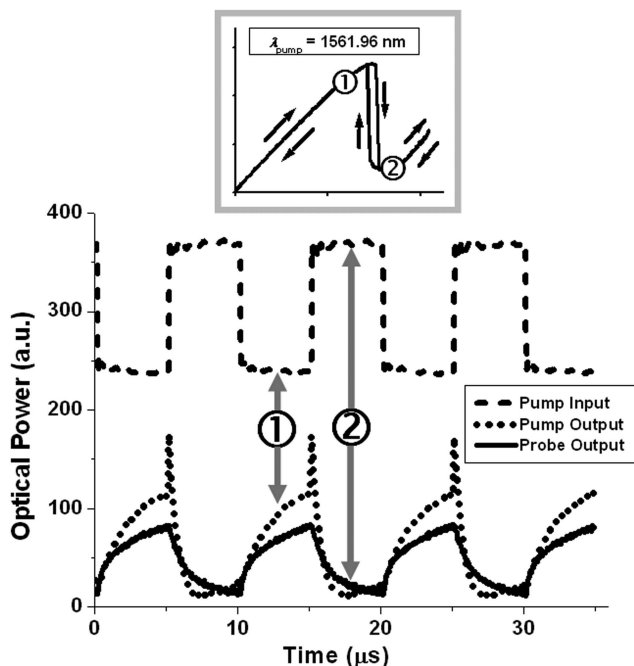


Fig. 5. All-optical switching on a pump-probe scheme with $\lambda_{\text{pump}} = 1561.96$ nm and $\lambda_{\text{probe}} = 1580.24$ nm at 100 kHz. Inset, hysteresis curve for $\lambda_{\text{pump}} = 1561.96$ nm. Markers show the points in the bistability curve between which the pump power is modulated: ① high-output state, ② low-output state.

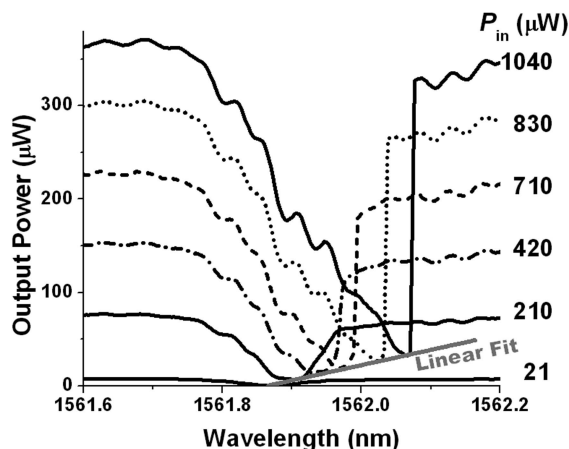


Fig. 6. Dependence of the quasi-TE transmission spectra on input power. The resonance shift shows good agreement with a linear absorption fit.

To determine the absorption mechanism inducing the thermo-optic effect, we measured the spectral transmission as a function of the pump power (Fig. 6). We found that the resonance shift shows a linear dependence, with a coefficient of 200 pm/mW. The linear absorption coefficient in the Si ring required to induce such a shift is $\alpha_L = (7.1 \pm 3.7)$ dB/cm. This value was assessed from (a) the estimated temperature increase ($\Delta T = 1.5^\circ\text{C}$) in the ring that is necessary for achieving such a resonance shift due to the thermo-optic effect,⁸ (b) numerical calculations of heat diffusion in the structure to estimate the power

necessary to achieve such a temperature increase, and (c) calculations of the optical intensity inside the ring. For comparison, we also estimated the nonlinear absorption coefficient in the ring; considering the largest output power $P_{\text{out}} = 370 \mu\text{W}$ (see Fig. 6), the highest possible power circulating in the ring at λ_{resA} should be $P_{\text{ring}} = 10^{IL/10} P_{\text{out}} (\text{FE})^2 = 60$ mW, where $\text{FE} = 7.2$ is the on-resonance field enhancement factor at λ_{resA} .¹⁰ For such an optical power, taking into account the calculated mode field profile in the ring core and a two-photon absorption coefficient of $\beta_{\text{TPA}} = 7.9 \times 10^{-12}$ m/W (Ref. 12), the nonlinear optical absorption coefficient in the ring core is $\alpha_{\text{NL,max}} = \beta_{\text{TPA}} I_{\text{avg}} = 0.13$ dB/cm, where I_{avg} is the average optical intensity inside the ring core. Note that the nonlinear absorption coefficient is much lower than its linear counterpart. Therefore the absorption mechanism is predominantly linear. This high linear absorption mechanism may arise from surface states due to a dangling bond created by the nonpassivated sidewalls.¹³

The authors acknowledge Roberto R. Panepucci regarding device fabrication and support from the Cornell Center for Nanoscale Systems funded by the National Science Foundation. This work was performed in part at the Cornell Nanoscale Science & Technology Facility, a member of the National Nanotechnology Infrastructure Network, which is supported by the National Science Foundation under grant ECS-9731293, its users, Cornell University, and industrial affiliates. V. R. Almeida acknowledges sponsorship from the Brazilian Defense Ministry. M. Lipson's e-mail address is lipson@ece.cornell.edu.

References

1. A. Liu, R. Jones, L. Liao, D. Samara-Rubio, D. Rubin, O. Cohen, R. Nicolaescu, and M. Paniccia, *Nature* **427**, 615 (2004).
2. R. L. Espinola, M.-C. Tsai, J. T. Yardley, and R. M. Osgood, Jr., *IEEE Photon. Technol. Lett.* **15**, 1366 (2003).
3. K. Wada, H. C. Luan, D. R. C. Lim, and L. C. Kimerling, *Proc. SPIE* **4870**, 437 (2002).
4. R. A. Soref and B. R. Bennett, *Proc. SPIE* **704**, 32 (1987).
5. H. M. Gibbs, *Optical Bistability: Controlling Light with Light* (Academic, Orlando, Fla., 1985).
6. S. D. Smith, *Appl. Opt.* **25**, 1550 (1986).
7. M. Warren, W. Gibbons, K. Komatsu, D. Sarid, D. Hendricks, H. M. Gibbs, and M. Sugimoto, *Appl. Phys. Lett.* **51**, 1209 (1987).
8. G. Cocorullo and I. Rendina, *Electron. Lett.* **28**, 83 (1992).
9. D. Sarid, *Opt. Lett.* **6**, 552 (1981).
10. V. Van, T. A. Ibrahim, P. P. Absil, F. G. Johnson, R. Grover, and P.-T. Ho, *IEEE J. Sel. Top. Quantum Electron.* **8**, 705 (2002).
11. V. R. Almeida, R. R. Panepucci, and M. Lipson, *Opt. Lett.* **28**, 1302 (2003).
12. M. Dinu, F. Quochi, and H. Garcia, *Appl. Phys. Lett.* **82**, 2954 (2003).
13. A. M. Agarwal, L. Liao, J. S. Foresi, M. R. Black, X. Duan, and L. C. Kimerling, *J. Appl. Phys.* **80**, 6120 (1996).